THE JOURNAL OF PHYSICAL CHEMISTRY B

ARTICLE

pubs.acs.org/JPCB

Surfactant Concentration Effects on Micellar Properties

Arben Jusufi,*,† David N. LeBard, Benjamin G. Levine,‡ and Michael L. Klein

Institute for Computational Molecular Science and Department of Chemistry, Temple University, Philadelphia, Pennsylvania 19122, United States

ABSTRACT: A hydrophobic theory is combined with a Debye–Hückel approximation to calculate surfactant micellization properties such as the critical micelle concentration (cmc) and concentration effects. The predictive power of the theory is validated by comparison with experimental data of various ionic surfactant types in presence of salt. The theory is also used to describe micellar properties of surfactant models developed for molecular simulations for which cmc computations become infeasible. The theory allows such computations and helps to evaluate the quality of models used in simulations.

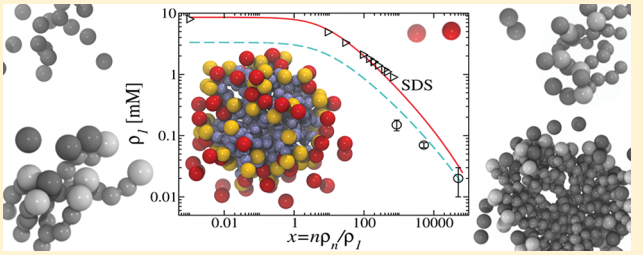

INTRODUCTION

The self-assembly of amphiphilic molecules plays an important role in natural and industrial applications, ranging from the formation of cell membranes to the development of surfactant detergent cleansers.[1−3] The driving force for self-assembly stems from the interplay between hydrophobic and hydrophilic interactions of the amphiphile. Depending on the molecular architecture and other conditions (presence of salt, temperature, etc.), surfactants form various aggregates of well-defined shapes above the critical micelle concentration (cmc). Micellar properties, such as the cmc, aggregation number (n) and shape have been studied extensively through experiments[2] and theory.[1,4−9] Combined, they delivered a robust understanding of the driving forces behind the self-assembly of surfactants and lipids. A useful tool to study micelle assembly is molecular simulations, which have been widely used in the past three decades.[8−14] One difficulty of simulations is determining micellization properties at surfactant concentrations nearing the cmc, or, to predict the cmc itself. Most surfactants with hydrocarbons chains more than eight carbons in length exhibit low cmc values (<10 mM), and the majority of computations required in the simulation would involve the motion of water molecules, instead of the motion of dissolved surfactants. Moreover, micellization processes require time scales of at least 1 μs,[15] a long period for molecular dynamics (MD) simulations in particular for MD simulation using fully atomistic models. Even with high performance simulations employing massively parallel computations, it is challenging to conduct such calculations. Simulations are therefore restricted to higher concentration regimes (>100 mM) from which it is difficult to predict properties at cmc conditions. In this high concentration regime the free monomer concentration (c_1) decreases and is therefore not identical to the cmc, particularly for ionic surfactants.[16] Only a few theories capture this behavior. Bales and co-workers outlined a semiempirical approach to estimate concentration effects on c_1.[16,17] A more fundamental picture was provided by Gunnarsson et al., who combined thermodynamic approaches with the Poisson–Boltzmann (PB) theory to predict cmc values and concentration effects on micellar properties of ionic surfactants, such as sodium dodecyl sulfate (SDS). Although the theory did not include self-consistent calculations of n, a weak drop of the free monomer concentration was predicted upon increasing total surfactant concentration (c_t) in a range of up to twice the calculated cmc (7 mM) of SDS.[4] This tendency is in line with experimental observations.[16,17]

Here, we provide a self-consistent approach with respect to c_1, n, and the micelle ionization degree α, formed from a Debye–Hückel (DH) approximation on top of a hydrophobic theory developed by Maibaum et al. to describe the micellization of nonionic surfactants.[7] We study the change in the free monomer concentration as c_t is increased from the cmc to many orders of magnitude above this value. We validate the model against experimental data reported in literature, and demonstrate how to predict the cmc for surfactant models used in MD simulations. The theoretical model is adjusted to a specific coarse-grained (CG) simulation model of sodium hexyl sulfate (S6S) based on a recently developed SDS CG model.[18] S6S is a computationally feasible surfactant type in MD due to its high cmc ≈420 mM.[19] The adjusted theoretical model was subsequently used to predict the cmc for related sodium alkyl sulfates (SmS) for which even CG MD simulations are unfeasible. For this purpose extensive MD simulations of SDS and S9S were performed to systematically study the change of c_1 with increasing $c_t \gg$ cmc. About 10^5 particles were simulated for over 100 μs on Graphics Processing Units; the details of these calculations will be presented elsewhere.[20] The adjusted theory provides cmc calculations for CG models of SDS and S9S. In this way the quality of molecular

Received: October 26, 2011
Revised: December 13, 2011
Published: December 16, 2011

ACS Publications © 2011 American Chemical Society

force fields used in simulations of surfactants could be tested with regard to their micellization properties.

THEORY

For the following theoretical model we assume that the micellar aggregates are of spherical shape and monodisperse with respect to the aggregation number n. According to Tanford's packing consideration,[1] which is supported by experimental observations,[21] the first assumption is a fair condition as long as $n \lesssim 100$. Further, we show below that significant deviations of theoretical calculations from experimental observations occur above that threshold. The free energy density of a mixture of free surfactants and micelles is comprised of the following terms:

$$F = S_1 + S_n + S_c + S_s + \rho_1 f_1 + \rho_n f_n + \rho_t \mu_t + \rho_s \mu_s \quad (1)$$

where $\rho_i = c_i/M_i$ is the number density of free surfactants $(i = 1)$ and micelles $(i = n)$, and M_i are the corresponding molar masses. The total surfactant density is $\rho_t = \rho_1 + n\rho_n$, and ρ_s denotes the salt ion density in solution. The first four terms in eq 1 account for the entropic free energy density contributions of free surfactants $(i = 1)$, micelles $(i = n)$, counterions $(i = c)$, and salt co-ions $(i = s)$, and are expressed through their ideal gas contribution only $\beta S_i = \rho_i[\ln(\rho_i a^3) - 1]$. Here, a sets a microscopic length scale of the system and corresponds to an effective hydrocarbon tail bead size; $\beta = 1/(kT)$ is the inverse thermal energy. Note that the counterion density is $\rho_c = \rho_1 + \alpha n\rho_n + \rho_s$. The latter term must be added here when salt ions are identical with surfactant counterions, e.g. Na^+ ions steming from SDS and from added NaCl. The ionization degree of a micelle with aggregation number n is defined through the number of counterions condensed on the micellar surface, N_c, yielding $\alpha = N_c/n$. Hence, from the available micellar counterions, only $\alpha n\rho_n$ worth contribute to the counterion entropy, while $(1 - \alpha)n\rho_n$ counterions are condensed on micelle surfaces. Furthermore, eq 1 contains internal free energy contributions of free surfactants f_1 and of micelles f_n (containing n aggregates). Finally, the chemical potentials μ_t and μ_s set the concentrations of surfactants and added salt, respectively. The free energy difference $\Delta G \equiv f_n - nf_1$ is considered as the driving force for self-assembly. The main task is to identify the main free energy contributions to ΔG. One can decompose this free energy density into a charge-neutral (ne) and an electrostatic (el) part, such that $\Delta G = \Delta G^{ne} + \Delta G^{el}$. The first term ΔG^{ne} has been evaluated by Maibaum et al., see eq 8 of ref 7. This term includes competing nonionic hydrophobic and hydrophilic free energy contributions that are sufficient for a realistic description of nonionic surfactant micelles.

$$\beta\Delta G^{ne} = -n\beta\Delta\mu + \beta g n^{2/3} + h n^{5/3} \quad (2)$$

The first term is the free energy of transfer of single alkanes from bulk water into bulk alkane solution and drives aggregation. It is estimated as $\Delta\mu = (7.96 + 3.22m)$ kJ/mol at room temperature $T = 298$ K that we used throughout this work. The linear dependence on the tail bead number m is valid as long as $m < 12$. The second and third term in eq 2 compete with the first hydrophobic contribution and account for free energy costs due to surface tension and the placement of the hydrophilic headgroups on the surface area of micellar aggregates, respectively. The constants g and h in eq 2 has been evaluated in ref 7 as well. Here we only give the results: $g = (36\pi)^{1/3}\gamma_{ow}a^2(\delta/a)^{2/3}$ with $\gamma_{ow} = 51$ mN/m being the oil-water interfacial tension, and $h = (3/(4\pi))^{2/3}(96/49)(a/\delta)^{4/3}$. Two length scales enter into these constants: An effective tail bead size a and an average tail length δ. Both quantities determine, together with n, the packing condition of a micelle, which leads to an explicit dependence of the micellar radius R on n: $R = (3\delta a^2/(4\pi))^{1/3}n^{1/3}$.[7] As for poly(ethylene glycol) surfactants, we keep $a = 0.3$ nm.[7] We replace, however, δ by the surfactant tail length and use the relationship $\delta = [0.154 + (m - 1)0.127]$ nm, which is an estimation based on the molecular architecture of linear hydrocarbon chains.[1]

The electrostatic free energy density contribution ΔG^{el} is estimated through a DH approximation. For the micelles a spherical geometry is assumed, which is a fair approximation for ionic micelles, since their aggregation numbers barely reach 100, above which ellipsoidal shapes are expected.[1,21] Only at high surfactant and salt concentrations is this limit reached, and only then do nonspherical aggregate shapes need to be considered. The electrostatic contribution is

$$\Delta G^{el} = U(\alpha n, R) - n[U(-1, r_s) + (1 - \alpha)U(1, r_c)] \quad (3)$$

Here, we use the well-known DH approximation for charging spherical particles of valency z to a radius r in a solvent of ions:[22] $\beta U(z,r) = z^2\lambda_B/[2r(1 + \kappa r)]$ with the Bjerrum length $\lambda_B = 0.72$ nm at room temperature and the inverse screening length $\kappa = (4\pi\lambda_B(2\rho_1 + \alpha n\rho_n + 2\rho_s))^{1/2}$ in which free surfactants, free counterions, and salt co-ions provide the electrostatic screening. Note that in eq 3 the cost of charging a micelle of valency αn is reduced by the electrostatic energy gain of eliminating charges steming from n ionic surfactant headgroups (of radius r_s) and $(1 - \alpha)n$ counterions (of radius r_c) in solution.[23]

Equations 2 and 3 are employed into the minimization of eq 1 using the definition $\Delta G \equiv f_n - nf_1$. The minimization of F was carried out simultaneously with respect to ρ_1, n, and α. In the following we restrict the focus of the discussion to the results of ρ_1. In contrast to charge-neutral surfactants, the solutions for ionic surfactants cannot be formulated in a closed form mainly due to the explicit dependence of $\kappa = \kappa(\rho_1,\alpha)$ and $R = R(n)$ that both enter into ΔG^{el}. Also note that in the minimization one has to account for $\rho_n = (\rho_t - \rho_1)/n$. Although the minimization must be performed numerically it is helpful to discuss the analytical equation for ρ_1:

$$\ln(\rho_1 a^3) = \frac{1}{2 - \alpha}\left[\beta\left(\frac{\Delta G}{n} - x\frac{\rho_1}{n}\frac{\partial \Delta G}{\partial \rho_1}\right) - (1 - \alpha)\ln\left(1 + \frac{\rho_s}{\rho_1} + \alpha x\right)\right] \quad (4)$$

where $x \equiv n\rho_n/\rho_1$. In the lower limit, $x \approx 0.01$,[4] most surfactants are free, and the lowest surfactant density at which micelles occur is defined as the cmc, i.e. $\rho_1 \approx \rho_{cmc}$ for $x \ll 1$. In the absence of salt $(\rho_s = 0)$ eq 4 simplifies to $\ln(\rho_{cmc}a^3) \approx \beta\Delta G/[(2 - \alpha)n]$ for $n \gg 1$. The factor $(2 - \alpha)$ in the denominator stems from free counterions. At $\alpha = 1$ the well-known exponential relationship between the cmc and the free energy for micellization is obtained.[1] The concentration effects can be readily seen from 4. As the surfactant concentration is increased, corresponding to $x = n\rho_n/\rho_1 = (\rho_t - \rho_1)/\rho_1 \gg 1$, the entropic counterion term—the last term in 4—as well as $\partial\Delta G/\partial\rho_1$ both become important. Here one can expect strong deviations of ρ_1 from ρ_{cmc}. Nonionic surfactants do not possess such contributions, and the free surfactant concentration remains constant and identical to the cmc.

dx.doi.org/10.1021/jp2102989 |J. Phys. Chem. B 2012, 116, 987–991

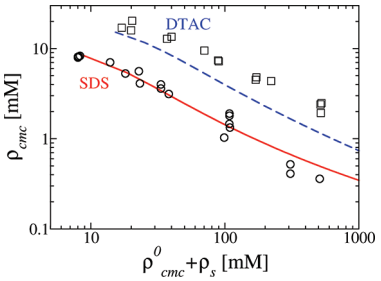

Figure 1. Experimental data (symbols) and theoretical predictions (lines) of the cmc for SDS (solid line, circles) and DTAC (dashed line, squares) as a function of added NaCl salt ρ_s. The abscissa is shifted by the cmc value in the absence of salt ρ^0_{cmc}. Experimental data are taken from refs 25−27 for SDS and from refs 24−28 for DTAC.

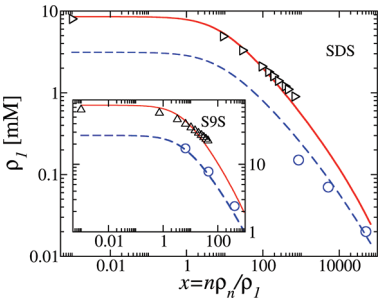

Figure 2. Free monomer concentration ρ_1 versus the surfactant concentration in micelles $n\rho_n$ relative to ρ_1. Shown are theoretical predictions (solid line) for SDS micelles and S9S micelles (inset) in comparison with results obtained from an empirical fit formula applied on experimental points (triangles);[17,29] see text for more details. Theoretical predictions (dashed line) of CG simulation results (circles) are also shown for SDS and for S9S (inset).

RESULTS

Before analyzing concentration effects, we validate the model against ρ_1 and the cmc for anionic SDS and cationic dodecyltrimethylammonium chloride (DTAC) surfactants. Results with respect to n and α are presented in the Appendix. For SDS and DTAC, the headgroup and counterion radii were taken from ref 14 and were included into eq 3. No adjustable parameters were used for these calculations. In the absence of salt we obtain ρ^0_{cmc} = 8.4 mM and n = 59 for SDS, and ρ^0_{cmc} = 15.2 mM and n = 52 for DTAC;[2] see Figure 1 for comparisons with experimental data. The theoretical value for DTAC lies slightly below the experimental range. Experimental aggregation numbers range from 50[19] to 64[16] for SDS, and are around 45 for DTAC.[19,24] We tested the salt dependence of the cmc ($\rho_s > 0$): Figure 1 shows reasonable agreement of the cmc for SDS in presence of NaCl salt. For DTAC the cmc is underestimated over a larger concentration range of added salt. As for SDS, the discrepancy increases with added salt. The main reason is that the DH approximation assumes spherical micelles. With increasing salt concentration, however, the micelles become more ellipsoidal.[1,21] Such morphological changes are not included in the theory, resulting in discrepancies as n approaches 100 (see the Appendix).

The effect of the total surfactant concentration ρ_t on ρ_1 becomes important when $x = n\rho_n/\rho_1 = (\rho_t - \rho_1)/\rho_1 \gg 1$ due to the terms in eq 4 that are factorized with x. As presented in Figure 2, ρ_1 drops significantly for $x \gg 1$. In turn, $\rho_1 \approx \rho_{cmc}$ holds

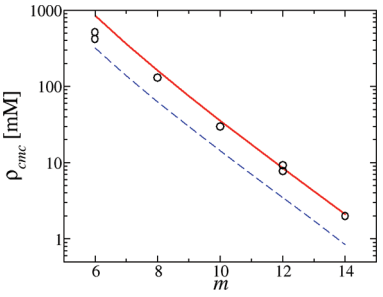

Figure 3. Experimental data (circles)[19,29,31] and theoretical prediction (solid line) of the cmc for various sodium alkyl sulfates SmS. Also shown is the predicted cmc using the CG parameter setting (dashed line).

below that threshold. The theoretical prediction is in good agreement with results obtained from fits of experimental data using a semiempirical formula. The calculation of eq 5 in ref 17 leads to the SDS values shown in Table 1 of ref 17. Those values are plotted here in Figure 2 (triangles). For S9S we used the same empirical equation to calculate the free monomer concentration using experimental values for cmc_0 = 64.6 mM, α = 0.574,[29] and a molar S9S volume of 0.246 L/mol (assuming a 1 g/mL density of S9S). The S9S results (triangles) are juxtaposed with data produced by our theoretical model (solid line) in the inset of Figure 2. As in the SDS case, the data from both models agree well over a large range of x. Note, however, that the empirical expression (eq 5 in ref 17) requires the knowledge of cmc_0 and α a priori, while our theoretical model self-consistently yields values of those properties. The drop of $\rho_1(x)$ for large x illustrates the difficulty in estimating the cmc through simulations of ionic surfactants. Simulations are typically performed at high surfactant concentrations in order to avoid the computation of an overwhelming number of solvent molecules. Under such conditions it is not justified to approximate $\rho_1 \approx \rho_{cmc}$, in contrast to nonionic surfactants. Extensive MD were performed based on a CG model of surfactants, water and counterions.[18] We measured ρ_1 and n of up to three points of $\rho_t \gg \rho_{cmc}$ (ρ_t = 130 mM, 363 mM, and 1005 mM) for S6S, S9S and SDS. For a fair comparison between theory and CG simulation results the former requires parameter adjustments. According to the CG mapping of the CG surfactant model[30] we estimate the theoretical tail length on the basis of the CG tail architecture (bond length and angles): $\delta_{CG} = [0.365 + (m_{CG} - 1)0.364]$ nm with m_{CG} being the number of CG tail beads (2 for S6S, 3 for S9S, and 4 for SDS). Another adjustment of the theory needed for describing CG simulation results concerns the ion sizes of the sulfate headgroups and sodium counterions. Instead of using the actual radii implemented in the CG simulations (0.22 nm for both ion types), we need to account for structural artifacts caused by the CG treatment of ions and water molecules. We found that the Coulomb behavior among ions is significantly compromised by CG water molecules over a large range of ionic separations (<1.5 nm), including an overestimation of solvation effects compared to real solutions at distances below 1 nm. The ionic radii in the DH model are set to $r_s = r_c$ = 0.13 nm, yielding ρ_1 = 110 mM that was obtained from CG MD simulations at x = 9.14 for S6S. The theory predicts n = 18 which compares well with the simulation results (n = 23). The same adjusted ionic radii were used for the prediction of $\rho_1(x)$ of CG S9S and CG SDS, as shown in Figure 2. The agreement between theory and CG simulation results is satisfactory. The large discrepancy between

dx.doi.org/10.1021/jp2102989 |J. Phys. Chem. B 2012, 116, 987–991

theory and simulation observed for SDS at 130 mM ($x \approx 850$) is likely attributable to equilibration issues. Omitting that point a maximum discrepancy of 30% is observed between theory and CG simulations for SDS at 363 mM ($x \approx 5200$). The theory was used to evaluate the cmc of computationally infeasible systems using MD. At low x, $\rho_1(x)$ converges to a single cmc value, which we have juxtaposed with experimental data in Figure 3. The graph also shows the theoretical predictions of the experimental cmc of SmS with the same parameter setting used to describe the SDS salt dependence of the cmc shown in Figure 1. The comparison of the CG and experimental cmc in Figure 3 shows that the CG results are up to 3-fold smaller, indicating a stronger driving force for micellization of the CG surfactant model due to inaccuracies in the CG forcefield. According to eq 4, the driving force, $\Delta G/[n(2 - \alpha)]$, of CG model surfactants is only larger than real surfactants by $kT \ln(3) \approx 1kT$.

SUMMARY

In summary, we present a theoretical model that could be used to reduce the necessary amount of computational time needed to calculate the cmc and associated properties from simulations. As demonstrated here, only a single reference system, S6S—a computationally feasible one—is needed to adjust a single fit parameter, the ionic radius. Using the same parameter set, cmc predictions are provided for related surfactant types, which are impractical to obtain from conventional MD simulations. In this way, the theoretical model could serve as an evaluation method used to improve molecular force field parameters and provide a more realistic description of micellization properties. The model will be expanded to longer tail and double chain surfactants and lipids, thus affording calculations of cmc values in the μM regime or below. In this concentration range many experimental methods for determining the cmc are pushed to their accuracy limits, and the theory presented here could be used for accurate calculations at such low concentrations.

APPENDIX

Figures 4−6 show theoretical predictions of the aggregation number n and degree of ionization α (insets) in comparison with experimental data taken from literature. The micellar properties are plotted as functions of various parameters: Salt concentration ρ_s (Figure 4), normalized surfactant concentration x (Figure 5), and surfactant tail length m (Figure 6).

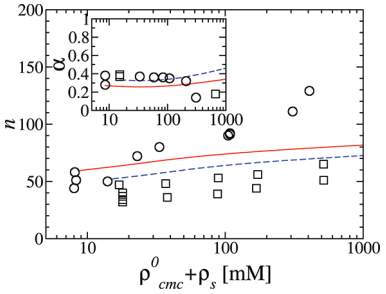

Figure 4. Experimental data (symbols) and theoretical predictions (lines) of the aggregation number n for SDS (solid line, circles) and DTAC (dashed line, squares) as a function of added NaCl salt ρ_s. The abscissa is shifted by the cmc value in the absence of salt ρ^0_{cmc} (8.4 mM for SDS, 15.2 mM for DTAC). Experimental data are taken from refs 25−27 for SDS and from refs 24−28 for DTAC. Inset: Theoretical prediction (lines) of the salt dependence of the degree of ionization α compared with experimental data for SDS[26,32] (circles) and for DTAC[33,34] (squares).

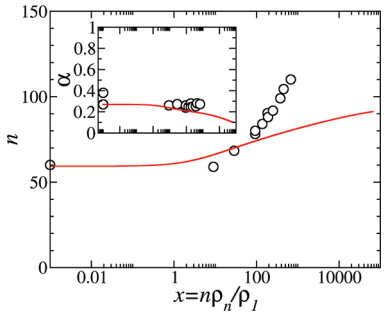

Figure 5. Aggregation number n and degree of ionization α (inset) versus the surfactant concentration in SDS micelles $n\rho_n$ relative to ρ_1. Theoretical predictions (solid line) of $n(x)$ in the absence of salt are compared to corresponding experimental data (circles).[17,26]

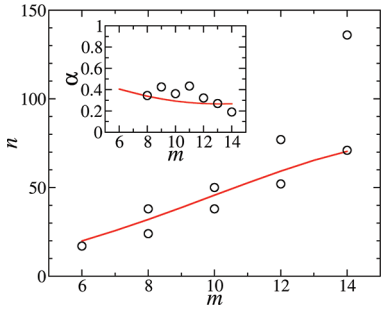

Figure 6. Experimental data (circles)[19,29,34−36] and theoretical prediction (solid line) of the aggregation number n and the degree of ionization α (inset) for various sodium alkyl sulfates SmS in the absence of salt. The theoretical properties are calculated at cmc conditions. The cmc values are plotted in Figure 3.

AUTHOR INFORMATION

Corresponding Author

*E-mail: arben.jusufi@csi.cuny.edu.

Present Addresses

[†]Department of Chemistry, College of Staten Island, City University of New York, NY

[‡]Department of Chemistry, Michigan State University, East Lansing, MI

ACKNOWLEDGMENT

The authors thank A. Z. Panagiotopoulos for helpful discussions. A.J. and M.L.K. are grateful for financial support from Procter & Gamble Research. Computer time (TG-MCA93S020) and hardware (CHE 09-46358) grants are also acknowledged.

REFERENCES

(1) Tanford, C. *The Hydrophobic Effect: Formation of Micelles and Biological Membranes*; John Wiley & Sons Inc: New York, 1973.

(2) Rosen, M. *Surfactants and Interfacial Phenomena*, 2nd ed.; John Wiley & Sons Inc: New York, NY, 1989.

(3) Israelachvili, J. N. *Intermolecular and Surface Forces*; Harcourt Brace: London, 1992.
(4) Gunnarsson, G.; Jönsson, B.; Wennerström, H. *J. Phys. Chem.* **1980**, *84*, 3114–3121.
(5) Puvvada, S.; Blankschtein, D. *J. Chem. Phys.* **1990**, *92*, 3710–3724.
(6) Nagarajan, R.; Ruckenstein, E. *Langmuir* **1991**, *7*, 2934–2969.
(7) Maibaum, L.; Dinner, A. R.; Chandler, D. *J. Phys. Chem. B* **2004**, *108*, 6778–6781.
(8) Stephenson, B. C.; Goldsipe, A.; Beers, K. J.; Blankschtein, D. *J. Phys. Chem. B* **2007**, *111*, 1025–1044.
(9) Stephenson, B. C.; Goldsipe, A.; Blankschtein, D. *J. Phys. Chem. B* **2008**, *112*, 2357–2371.
(10) Jonsson, B.; Edholm, O.; Teleman, O. *J. Chem. Phys.* **1986**, *85*, 2259–2271.
(11) Watanabe, K.; Ferrario, M.; Klein, M. L. *J. Phys. Chem.* **1988**, *92*, 819–821.
(12) MacKerell, A. D., Jr. *J. Phys. Chem.* **1995**, *99*, 1846–1855.
(13) Sammalkorpi, M.; Karttunen, M.; Haataja, M. *J. Phys. Chem. B* **2007**, *111*, 11722–11733.
(14) Jusufi, A.; Hynninen, A.-P.; Panagiotopoulos, A. Z. *J. Phys. Chem. B* **2008**, *112*, 13783–13792.
(15) Alexandridis, P.; Holzwarth, J. F.; Hatton, T. A. *Langmuir* **1993**, *9*, 2045–2052.
(16) Quina, F. H.; Nassar, P. M.; Bonilhaf, J. B. S.; Bales, B. L. *J. Phys. Chem.* **1995**, *99*, 17028–17031.
(17) Bales, B. L. *J. Phys. Chem. B* **2001**, *105*, 6798–6804.
(18) Shinoda, W.; DeVane, R. H.; Klein, M. L. *Soft Matter* **2011**, *7*, 6178–6186.
(19) Zana, R. *Surfactant Science Series*; CRC Press: Boca Raton, FL, 2005; Vol. 125.
(20) LeBard, D. N.; Levine, B. G.; Mertmann, P.; Barr, S.; Jusufi, A.; Sanders, S.; Klein, M. L.; Panagiotopoulos, A. Z. *Soft Matter* **2012**, DOI: 10.1039/C1SM06787G.
(21) Bergström, M.; Pedersen, J. S. *Phys. Chem. Chem. Phys.* **1999**, *1*, 4437–4446.
(22) Levin, Y. *Rep. Prog. Phys.* **2002**, *65*, 1577–1632.
(23) Srinivasan, V.; Blankschtein, D. *Langmuir* **2003**, *19*, 9932–9945.
(24) Roelants, E.; De Schryver, F. C. *Langmuir* **1987**, *3*, 209–214.
(25) Hunter, R. J. *Foundations of Colloid Science*; Clarendon Press: Oxford, U.K., 1987; Vol. 1.
(26) Thévenot, C.; Grassl, B.; Bastiat, G.; Binana, W. *Colloids Surf., A* **2005**, *252*, 105–111.
(27) Umlong, I. M.; Ismail, K. *Colloids Surf., A* **2007**, *299*, 8–14.
(28) Emerson, M. F.; Holtzer, A. *J. Phys. Chem.* **1967**, *71*, 1898–1907.
(29) Ranganathan, R.; Tran, L.; Bales, B. L. *J. Phys. Chem. B* **2000**, *104*, 2260–2264.
(30) Shinoda, W.; DeVane, R. H.; Klein, M. L. *Mol. Simul.* **2007**, *33*, 27–36.
(31) Suárez, M. J.; López-Fontán, J. L.; Sarmiento, F.; Mosquera, V. *Langmuir* **1999**, *15*, 5265–5270.
(32) Shanks, P. C.; Franses, E. I. *J. Phys. Chem.* **1992**, *96*, 1794–1805.
(33) Drummond, C. J.; Grieser, F.; Healy, T. W. *Chem. Phys. Lett.* **1987**, *140*, 493–498.
(34) Bales, B. L.; Zana, R. *J. Phys. Chem. B* **2002**, *106*, 1926–1939.
(35) Nishikido, N. J. *Colloid Interface Sci.* **1983**, *92*, 588–591.
(36) Ogino, K.; Kakihara, T.; Abe, M. *Colloid Polym. Sci.* **1987**, *265*, 604–612.